

This manuscript has been co-authored by UT-Battelle, LLC under Contract No. DE-AC05-00OR22725 with the U.S. Department of Energy. The United States Government retains and the publisher, by accepting the article for publication, acknowledges that the United States Government retains a non-exclusive, paid-up, irrevocable, world-wide license to publish or reproduce the published form of this manuscript, or allow others to do so, for United States Government purposes. The Department of Energy will provide public access to these results of federally sponsored research in accordance with the DOE Public Access Plan (<http://energy.gov/downloads/doe-public-access-plan>).

# One-Dimensional All-Inorganic Copper Halides with Ultrabright Blue Emission and Up-Conversion Photoluminescence

*Tielyr Creason,<sup>1†</sup> Aymen Yangui,<sup>1†</sup> Rachel Roccanova,<sup>1</sup> Amanda Strom,<sup>2</sup> Mao-Hua Du,<sup>3</sup> and Bayrammurad Saparov<sup>1\*</sup>*

T. Creason, Dr. A. Yangui, R. Roccanova, Dr. B. Saparov  
Department of Chemistry and Biochemistry, University of Oklahoma, 101 Stephenson Parkway,  
Norman, OK 73019, United States

E-mail: [saparov@ou.edu](mailto:saparov@ou.edu)

Dr. A. Storm

Materials Research Laboratory, University of California, Santa Barbara, Santa Barbara,  
California 93106, United States

Dr. M-H. Du

Materials Science & Technology Division, Oak Ridge National Laboratory, Oak Ridge,  
Tennessee 37831, United States

<sup>†</sup>These authors contributed equally

**Keywords:** 1D metal halide, Pb-free halides, blue-emitting materials, up-conversion photoluminescence

All-inorganic metal halides such as Cs<sub>4</sub>PbX<sub>6</sub> and CsPbX<sub>3</sub> (X = Cl, Br, I) are attracting global attention owing to their promise in optoelectronic applications. However, the presence of the toxic heavy metal lead (Pb) in these materials is a major concern. Here, we report a family of nontoxic high-efficiency blue-emitting all-inorganic halides Rb<sub>2</sub>CuX<sub>3</sub> (X = Br, Cl), which exhibit one-dimensional crystal structures featuring anionic  $\infty[\text{CuX}_3]^{2-}$  ribbons separated by Rb<sup>+</sup> cations. The measured record high photoluminescence quantum yield values range from 64% to 100% for Rb<sub>2</sub>CuBr<sub>3</sub> and Rb<sub>2</sub>CuCl<sub>3</sub>, respectively. Furthermore, the measured emission linewidths are quite narrow with full width at half maximum (FWHM) values of 54 and 52 nm for Rb<sub>2</sub>CuBr<sub>3</sub> and Rb<sub>2</sub>CuCl<sub>3</sub>, respectively. Single crystals of Rb<sub>2</sub>CuCl<sub>3</sub> show an anti-Stokes photoluminescence (ASPL) signal, shown for the first time for Pb-free metal halides. Our discovery of highly-efficient narrow blue emitters based on a nontoxic and inexpensive metal

copper paves a way for the consideration of low-cost and environmentally-friendly copper halides for practical applications.

The United States Department of Energy (DOE) projects an estimated energy cost savings of \$630 billion from 2015 to 2035 if reliable solid-state lighting technologies can be developed and DOE goals are met.<sup>[1]</sup> For the cost-effective implementation of light-emitting diodes (LEDs), development of new inexpensive light emitters is an urgent need. Owing to their outstanding photophysical properties including tunable band gaps and emission colors, high photoluminescent quantum yields (PLQY) and excellent color purity, metal halide perovskite LEDs (PeLEDs) have been attracting increased attention in recent years.<sup>[2]</sup> Thus, high external quantum efficiency (EQE) green and near-infrared (NIR) light-emitting PeLEDs have already been developed including a recent report of a NIR-emitting PeLED with a high EQE of 21.6%.<sup>[3]</sup> However, the development of efficient blue-emitting halides has historically lagged behind, although recent reports show some progress in this area.<sup>[2]</sup> Notable examples include highly efficient blue emission with PLQY over 70% from CsPbBr<sub>3</sub> and its mixed analog CsPb(Br/Cl)<sub>3</sub>,<sup>[4]</sup> Cu<sup>2+</sup>-doped CsPb<sub>1-x</sub>Cu<sub>x</sub>X<sub>3</sub> (X = Br, Cl) quantum dots,<sup>[5]</sup> and from exfoliated crystals of (C<sub>6</sub>H<sub>5</sub>CH<sub>2</sub>NH<sub>3</sub>)<sub>2</sub>PbBr<sub>4</sub>.<sup>[2a]</sup> These materials have also been incorporated into blue PeLEDs with external quantum efficiency (EQE) values up to 1.5% for PEA<sub>2</sub>A<sub>n-1</sub>Pb<sub>n</sub>X<sub>3n+1</sub><sup>[2b]</sup> and 9.5% for Cs<sub>x</sub>FA<sub>1-x</sub>PbBr<sub>3</sub>.<sup>[6]</sup> Despite the remarkable progress in the last few years, these deep blue emitters are predominantly low-dimensional or nanostructured lead halide perovskites, which usually suffer from the lead toxicity and poor stability.<sup>[2]</sup> In principle, other Pb-free low-

dimensional halides should also demonstrate increased charge localization and enhanced excitonic properties observed in lead halide perovskites, yielding efficient blue emitters that are free of toxic Pb such as in the case of recently reported copper halides  $\text{Cs}_3\text{Cu}_2\text{X}_5$  and  $\text{CsCu}_2\text{X}_3$ .<sup>[7]</sup> In this work, we provide further evidence of the validity of this conjecture through preparation of all-inorganic nontoxic  $\text{Rb}_2\text{CuX}_3$  ( $\text{X} = \text{Cl}, \text{Br}$ ), which exhibit near-unity PLQY blue emission. The remarkably high PLQY demonstrated by these compounds is attributed to the creation of self-trapped excitons (STEs) within their one-dimensional (1D) crystal structure. Moreover, for  $\text{Rb}_2\text{CuCl}_3$ , our preliminary results indicate a net phonon-assisted anti-Stokes photoluminescence (ASPL), and an optical cooling efficiency of  $\sim 32\%$  at room temperature. Note that optical cooling by ASPL (also known as upconversion PL) was previously reported in several rare earth-based materials,<sup>[8]</sup> semiconductors such as  $\text{CdS}$ <sup>[9]</sup> and more recently in a few hybrid organic-inorganic<sup>[10]</sup> and all-inorganic perovskites type materials.<sup>[11]</sup> This process takes place as a result of a light excitation energy below the band gap of the material producing a non-equilibrium electron distribution. Then, the exciting photon first interacts with the lattice leading to phonon absorption followed by blue-shifted luminescence. This mechanism leads to the extraction of the heat energy from the lattice by emitting a higher energy photon, which cools down the material. The advantages of metal halides is their high PLQY photoemission properties and the relatively low trap-states density which are important parameters for optical cooling.<sup>[12]</sup> For example, exceptionally strong ASPL and a remarkable optical cooling of 58.7 K was observed in the exfoliated crystals of two-dimensional (2D) layered perovskite  $(\text{C}_6\text{H}_5\text{C}_2\text{H}_4\text{NH}_3)_2\text{PbI}_4$ .<sup>[10a]</sup>

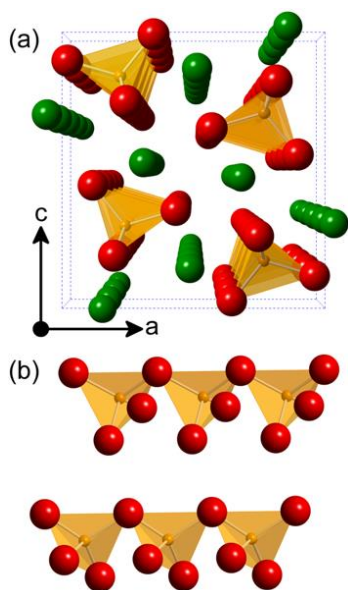


**Figure 1.** (a) A polyhedral view of the structure of  $\text{Rb}_2\text{CuX}_3$  projected along the  $b$ -axis, and (b) a close-up view of a segment of  ${}^\infty[\text{CuX}_3]^{2-}$  chains showing the corner-sharing connectivity of the  $\text{CuX}_4$  tetrahedra. Rb, Cu, and X are shown in green, yellow, and red, respectively.

$\text{Rb}_2\text{CuX}_3$  ( $\text{X} = \text{Br}, \text{Cl}$ ) crystallize in the orthorhombic space group  $\text{Pnma}^{[13]}$  featuring 1D  ${}^\infty[\text{CuX}_3]^{2-}$  chains separated by  $\text{Rb}^+$  cations (Figure 1, Table S1, Supporting Information (SI)). The anionic of  ${}^\infty[\text{CuX}_3]^{2-}$  chains are made of corner-sharing  $[\text{CuX}_4]$  tetrahedra along the  $b$ -axis.  $\text{Rb}_2\text{CuX}_3$  can be prepared both as polycrystalline powder samples or grown as single crystals using solid-state synthesis and solvent evaporation techniques, respectively (Figures S1-3). The presence of monovalent  $\text{Cu}^+$  cations in these materials and their ionic nature makes them susceptible to degradation in ambient air (Figures S4-S6, see SI for further details) However, larger single crystals of  $\text{Rb}_2\text{CuCl}_3$  do not exhibit any noticeable degradation when left in ambient air (Figure S6). On the other hand, our thermogravimetric analysis (TGA) measurements suggest that unlike most hybrid organic-inorganic lead halide perovskites,  $\text{Rb}_2\text{CuX}_3$  show no significant weight loss up to  $475^\circ\text{C}$  (Figure S7), which is in agreement with the reports of improved thermal stability of all-inorganic metal halides such as  $\text{Cs}_3\text{Cu}_2\text{Br}_{5-x}\text{I}_x$ ,<sup>[7a]</sup>  $\text{Rb}_4\text{Ag}_2\text{BiBr}_9$ ,<sup>[14]</sup> and  $\text{Cs}_2\text{SnI}_6$ .<sup>[15]</sup>

Differential scanning calorimetry (DSC) data show that  $\text{Rb}_2\text{CuCl}_3$  and  $\text{Rb}_2\text{CuBr}_3$  have peritectic decompositions at 274 and 271 °C, respectively, consistent with the reported phase diagrams.<sup>[16]</sup>

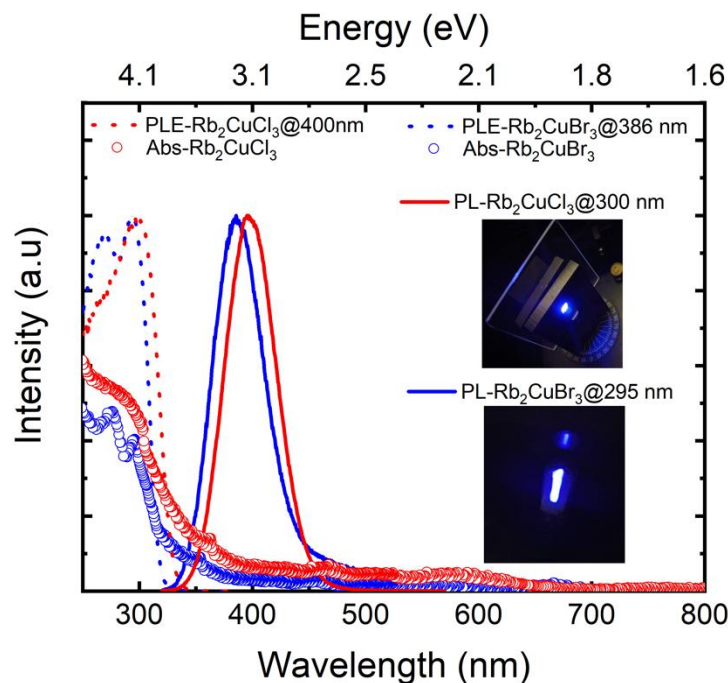


**Figure 2.** Room temperature optical absorption (circles), PLE (dashed lines) and PL (solid lines) of polycrystalline powders of  $\text{Rb}_2\text{CuBr}_3$  (blue) and  $\text{Rb}_2\text{CuCl}_3$  (red). The inset show the bright blue emission under UV irradiation.

Optical absorption spectra of polycrystalline powder samples of  $\text{Rb}_2\text{CuX}_3$  show two features at  $\sim 276$  and  $\sim 300$  nm. Upon UV irradiation, the room temperature PL spectra of polycrystalline powders of  $\text{Rb}_2\text{CuX}_3$  show a very bright blue emission (Figure 2). The PL maxima are located at  $\sim 385$  and  $395$  nm, with full width at half maximum (FWHM) values of 54 and 52 nm and relatively small Stokes shifts of 85 and 93 nm for  $\text{Rb}_2\text{CuBr}_3$  and  $\text{Rb}_2\text{CuCl}_3$ , respectively. Usually, low-dimensional (1D and 0D) metal halides materials emit strongly Stokes shifted spectra due to significant structural distortions in excited states.<sup>[17]</sup> In contrast, our PL results on  $\text{Rb}_2\text{CuX}_3$  are notably different for several reasons. First,  $\text{Rb}_2\text{CuX}_3$  are among the few blue

emitters with a near UV excitation and relatively small Stokes shift blue emission,<sup>[18]</sup> which is advantageous given the small energy loss between photoluminescence excitation (PLE) and emission (PL) spectra. Secondly, the measured PL linewidths of 54 and 52 nm for  $\text{Rb}_2\text{CuBr}_3$  and  $\text{Rb}_2\text{CuCl}_3$ , respectively, are among the lowest for highly-efficient blue emitting bulk samples.<sup>[2a]</sup> Note that obtaining materials that combine efficient blue emission with narrow emission linewidth is a recognized challenge, and the best literature-reported narrow blue emitters are  $(\text{C}_6\text{H}_5\text{CH}_2\text{NH}_3)_2\text{PbBr}_4$  nanoplates and  $\text{CsPbX}_3$  quantum dots, which unlike our bulk samples are obtained through nanostructuring.<sup>[2a]</sup> Finally, the visibly bright blue emission is corroborated by the high PLQY values of 64 and 85 % measured on polycrystalline powders of  $\text{Rb}_2\text{CuBr}_3$  and  $\text{Rb}_2\text{CuCl}_3$ , respectively (see Figure S8a, b). PLE spectra measured on polycrystalline  $\text{Rb}_2\text{CuX}_3$  for emission wavelengths of 386 and 400 nm show maxima at 295 and 300 nm, accompanied with a shoulder at 270 and 265 nm for  $\text{Rb}_2\text{CuBr}_3$  and  $\text{Rb}_2\text{CuCl}_3$ , respectively, which coincide with the measured absorption spectra (see Figure 2). Furthermore, we also measured room temperature PL/PLE on single crystals of  $\text{Rb}_2\text{CuCl}_3$ , which match the PL/PLE of the bulk powder sample (see Figure S9). Importantly, a unity ( $\sim 100\%$ ) PLQY value was measured on single crystals of  $\text{Rb}_2\text{CuCl}_3$  (see Figure S8c), which is the record high for known blue emitters.<sup>[2a,</sup>  
<sup>7a]</sup> The difference in the measured PLQY values with respect to the nature of sample (i.e., PLQY of 85% for a powder sample vs 100% for single crystals) is mainly due to the fact that single crystals contain less surface defects than polycrystalline powders and thin films. This is also consistent with the literature results on other copper halides<sup>[19]</sup> including PLQY values of 60% and 90% reported for thin films and single crystals of  $\text{Cs}_3\text{Cu}_2\text{I}_5$ , respectively.<sup>[7a]</sup> However, despite record high PLQY value for  $\text{Rb}_2\text{CuCl}_3$ , its photostability must be further improved for

device considerations as our periodic measurements of PLQY under continuous irradiation at its  $PLE_{\max}$  yielded  $\sim 75\%$  loss in PLQY in 1 hour (see Figure S10).

To understand the photophysical origin of the highly efficient blue-emission of  $Rb_2CuX_3$ , we measured its excitation and power dependence PL spectra at ambient temperature (see Figures S11-S12). Results show that  $Rb_2CuX_3$  compounds have excitation-dependent emission shapes and a linear dependence of the PL intensity as a function of excitation power. This fact suggests the intrinsic nature of  $Rb_2CuX_3$  blue emission, and the absence of saturation at high excitation power excludes the presence of permanent defects emissions.<sup>[14, 20]</sup> Therefore, we attribute this intense blue-emission to STEs often observed in metal halide all-inorganic systems.<sup>[7a, 14, 19, 21]</sup> Based on our single exponential fitting of the time-resolved PL data for  $Rb_2CuCl_3$  single crystals (Figure S13), a decay lifetime of 12.21  $\mu s$  was extracted. Long lifetime emission from STEs have also been reported for other metal halides including the related  $Cs_3Cu_2I_5$ . On the other hand, PL of  $Rb_2CuX_3$  can also be compared to that of binary copper halides.<sup>[19]</sup> It has been previously reported that  $\gamma$ -CuX ( $X = Br, Cl$ ) have significant light emission properties in the 300-400 nm spectral range, suitable for novel UV/blue light applications.<sup>[22]</sup> Here, we also measured the room temperature emission spectra of  $\gamma$ -CuX (Figure S14), that show a UV-blue light emission with the presence of two PL peaks at 384 and 395 nm for  $\gamma$ -CuCl and at 422 and 433 nm for  $\gamma$ -CuBr, in agreement with the previous reports.<sup>[22a, 23]</sup> However, the measured PLQY values of  $\gamma$ -CuX are very low ( $< 0.5\%$ ). The remarkable enhancement of emission efficiency of the ternary halides  $Rb_2CuX_3$  compared to the binary parents CuX is mainly due to the quantum confinement effect resulting from the reduction of structural dimensionality from 3D corner-sharing tetrahedra for  $\gamma$ -CuX (the zincblende structure) to 1D for  $Rb_2CuX_3$ , a well-known effect that results in higher exciton binding energies ( $E_b$ ) and improved exciton stabilities.<sup>[24]</sup> Here, based on the optical



absorption measurements for  $\text{Rb}_2\text{CuCl}_3$  (Figure 2), the exciton binding energy could be estimated as  $E_b = E_g - E_{\text{ex}} = 390 \text{ meV}$ ,<sup>[25]</sup> where  $E_g = 4.49 \text{ eV}$  and  $E_{\text{ex}} = 4.10 \text{ eV}$  are the band gap energy and the exciton energy, respectively. The high  $E_b$  values are characteristic of low dimensional metal halide materials.<sup>[7b, 24e, 26]</sup>

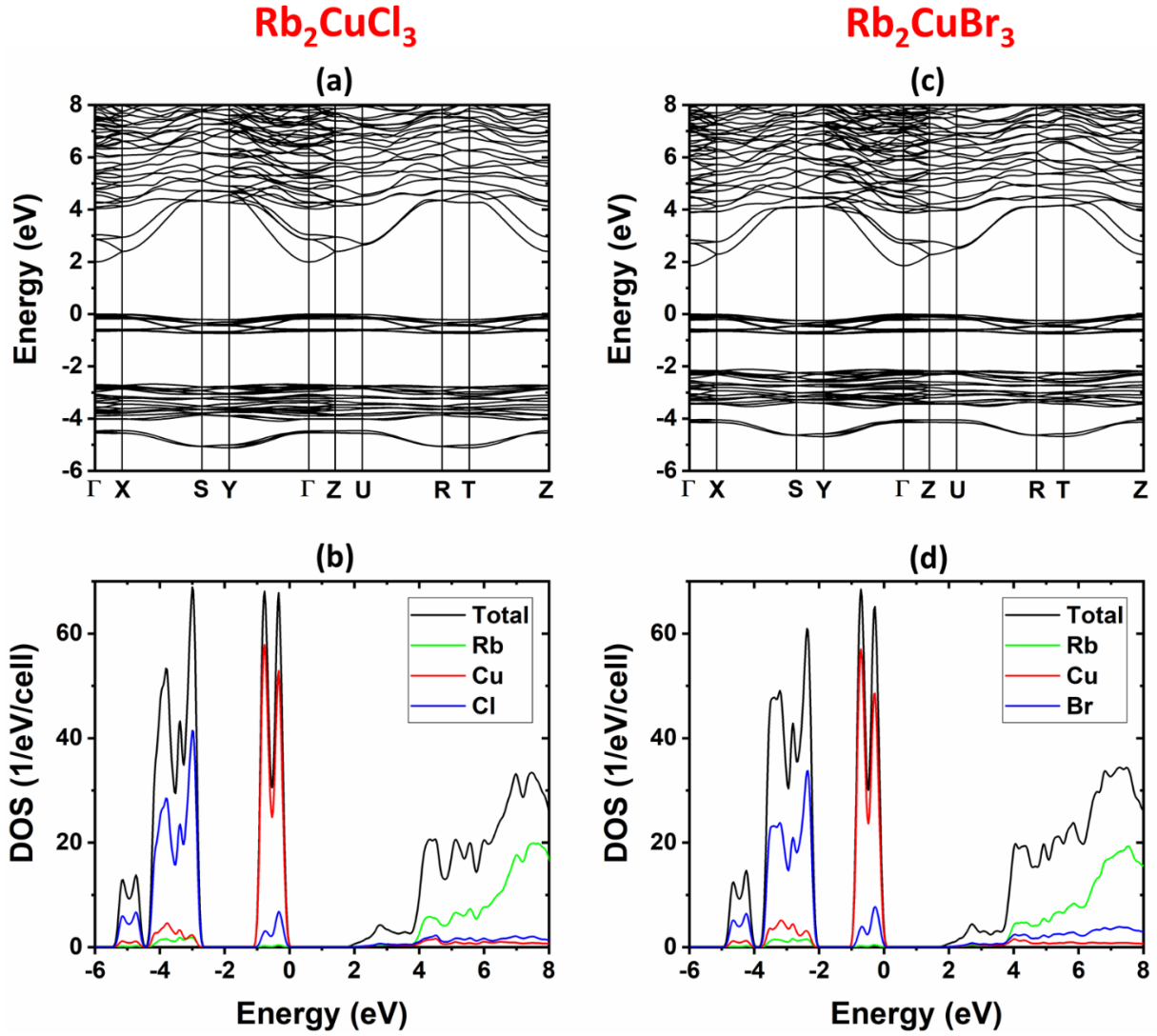


**Figure 3.** Electronic band structure and density of states (DOS) for (a-b)  $\text{Ru}_2\text{CuCl}_3$  and (c-d)  $\text{Ru}_2\text{CuBr}_3$ . Note that the band gaps are underestimated due to the band gap error in the PBE calculation.

To further investigate the main origin of the ultrabright blue emission of  $\text{Rb}_2\text{CuX}_3$ , we carried out DFT calculations (SI). Figure 3 shows the calculated electronic band structure and density of

states (DOS) plots.  $\text{Rb}_2\text{CuBr}_3$  has a direct band gap at the  $\Gamma$  point. In contrast, the band gap of  $\text{Rb}_2\text{CuCl}_3$  is slightly indirect – the conduction band minimum (CBM) is at the  $\Gamma$  point while the valence band maximum (VBM) is located between the  $\Gamma$  and the Z points. However, the top of the valence band between the  $\Gamma$  and the Z points is extremely flat as can be seen in Figure 3a; the energy of the top valence band is changed by only 0.002 eV from the  $\Gamma$  point to the VBM, which is negligible. Thus, the band gap of  $\text{Rb}_2\text{CuCl}_3$  is nearly direct. The DOS projected to each atomic species (Figures 3b-d) shows that the valence band is mainly made up of Cu-3d orbitals hybridized with halogen p orbitals while the conduction band has a mixed character of Cu-4s, Rb-5s, and halogen-p. The valence band is narrow, resulting from the localized nature of Cu-3d orbitals, while the conduction band is dispersive not only along the 1D chain direction (Y axis) but also along directions perpendicular to the chain. Thus, the electronic structure of  $\text{Rb}_2\text{CuCl}_3$  and  $\text{Rb}_2\text{CuBr}_3$  do not have the 1D character.

The calculated band gaps of  $\text{Rb}_2\text{CuCl}_3$  and  $\text{Rb}_2\text{CuBr}_3$  are 1.99 eV and 1.85 eV, respectively, which are expected to be underestimated due to the well-known band gap error in the PBE calculation but are consistent with previous PBE calculations.<sup>[27]</sup> Since the valence bands of both halides have mainly the Cu-3d character, their band gaps are weakly dependent on the type of the halogen atom. The Br-4p band in  $\text{Rb}_2\text{CuBr}_3$  is closer in energy to the Cu-3d band than the Cl-3p band in  $\text{Rb}_2\text{CuCl}_3$ , thus having a stronger hybridization with the Cu-3d band. As a result, the Cu-3d band in  $\text{Rb}_2\text{CuBr}_3$  is pushed up higher than that in  $\text{Rb}_2\text{CuCl}_3$ , resulting in a higher VBM and a slightly smaller band gap.

We further studied excitonic properties using more advanced PBE0 calculations which provide much improved description of the band gap and charge localization in insulators. Since the electronic structures of  $\text{Rb}_2\text{CuCl}_3$  and  $\text{Rb}_2\text{CuBr}_3$  have the similar characteristics as shown in

Figure 3, we focus on the exciton in  $\text{Rb}_2\text{CuCl}_3$ . The PBE0 calculation increases the band gap of  $\text{Rb}_2\text{CuCl}_3$  at the  $\Gamma$  point to 4.51 eV, which present a good agreement with the experimental band gap estimated based on the optical absorption data shown in Figure 2. The excited-state structural relaxation leads to a strong local structural distortion. The resulting localized STE is shown in Figure S15. The exciton self-localization around a Cu ion on the 1D Cu-Cl chain significantly weakens two Cu-Cl bonds (Cu(1)-Cl(1) and Cu(1)-Cl(2) in Figure S15). The calculated Cu(1)-Cl(1) and Cu(1)-Cl(2) bond lengths are 2.85 Å and 2.61 Å, which are 16.3% and 6.5% longer than the Cu-Cl bond length of 2.45 Å at the ground state. The calculated exciton emission energy based on the relaxed STE structure is 2.88 eV, close to the experimentally measured peak emission energy (3.14 eV or 395 nm). The good agreement between the calculated and measured exciton excitation/emission energies validates the excited-state theoretical modeling and supports the predicted exciton self-trapping as shown in Figure S15.

For  $\text{Rb}_2\text{CuCl}_3$ , the unity PLQY blue emission and noticeable overlap between the absorption and emission spectra (see Figure 2) suggest a possible optical cooling due to PL upconversion.<sup>[8, 10a]</sup> As shown in Figure 2, the optical absorption spectra of  $\text{Rb}_2\text{CuX}_3$  show a long band tail that quenches only at a very low energy ( $\sim 1.9$  eV), suggesting a high probability to have phonon-assisted ASPL above the 1.9 eV (650 nm) energy. As a preliminary study, we measured the ASPL spectra of the highly emissive single crystals of  $\text{Rb}_2\text{CuCl}_3$  using different excitation wavelengths in the 490-650 nm range (Figure 4). Results show the presence of upconversion PL with the maximum emission observed under 520 nm excitation. Note that the other possible mechanisms of ASPL include defect/impurity effects and two-photon absorption. However, since the lowest excitation peak is observed at 300 nm, the two-photon absorption mechanism would necessitate  $\text{PLE}_{\text{max}}$  of 600 nm for ASPL instead of the observed 520 nm. The defect effects are

largely ruled out based on the observed unity PLQY for the  $\text{Rb}_2\text{CuCl}_3$  single crystals, which have also been shown to be free of impurities using the X-ray methods (SI).

According to the previous studies based on Sheik-Bahae theory,<sup>[8, 10a, 11, 28]</sup> the optical cooling efficiency can be estimated from the following equation:

$$\eta_C = \eta_{PL} \frac{E_{em}}{E_{ex}} - 1,$$

where  $\eta_C$  and  $\eta_{PL}$  are the cooling and PL efficiency, respectively, and  $E_{em}$  and  $E_{ex}$  present the emission and excitation energies. Considering the fact that single crystals of  $\text{Rb}_2\text{CuCl}_3$  shows a 100% PLQY, and the maximum ASPL occurs at 395 nm (3.14 eV) under 520 nm (2.385 eV), using the above equation, an optical cooling efficiency of  $\sim 32\%$  is estimated. This value is similar to the highest values recently reported for hybrid perovskite<sup>[10a, 29]</sup> and all inorganic metal halides.<sup>[11, 30]</sup> Further detailed spectroscopic investigations including Raman spectroscopy is in progress to better understand the physical origin of the observed ASPL of  $\text{Rb}_2\text{CuCl}_3$ .

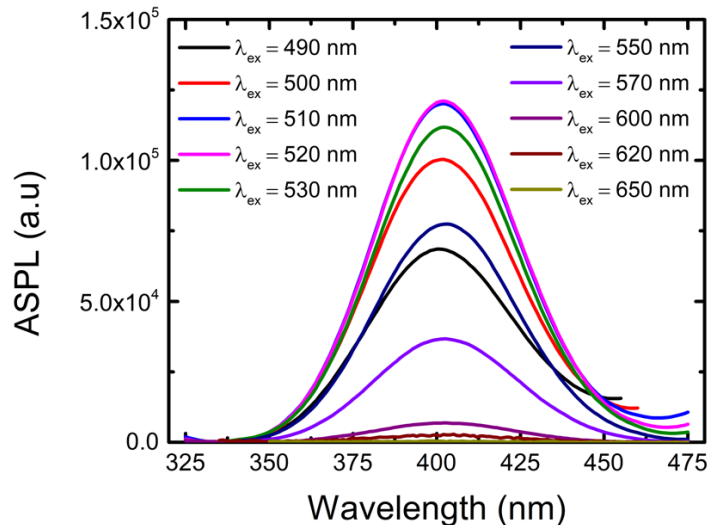


**Figure 4.** Anti-Stokes photoluminescence spectra of a  $\text{Rb}_2\text{CuCl}_3$  single crystal measured at ambient temperature and for different excitation wavelengths.

In summary, we report the photophysical properties of bulk and single crystal samples of all-inorganic metal halide materials  $\text{Rb}_2\text{CuX}_3$  ( $\text{X} = \text{Br}, \text{Cl}$ ), which exhibit one-dimensional crystal structures featuring anionic  ${}^1_{\infty}[\text{CuX}_3]^{2-}$  ribbons separated by  $\text{Rb}^+$  cations. These materials simultaneously show remarkably high blue emission efficiency and narrow emission linewidths: PLQY values of 64% to 100% and FWHM values of 54 and 52 nm for  $\text{Rb}_2\text{CuBr}_3$  and  $\text{Rb}_2\text{CuCl}_3$ , respectively, are among the record values in each category for bulk samples. Furthermore, the measured Stokes shifts of 85 and 93 nm for  $\text{Rb}_2\text{CuBr}_3$  and  $\text{Rb}_2\text{CuCl}_3$ , respectively, are unusually small for low-dimensional multinary halides, and can be advantageous for practical applications given the comparatively low energy loss between emission and excitation. Based on excitation-, time- and power-dependent PL studies, the physical origin of the emission is attributed to STEs, which is further supported by DFT calculations suggesting the presence of enhanced excitonic interactions. Moreover,  $\text{Rb}_2\text{CuCl}_3$  shows an ASPL that could provide up to 32% optical cooling efficiency, shown for the first time for Pb-free metal halides in this work. Importantly, discoveries of highly-efficient blue emitters based on nontoxic and inexpensive copper paves a way for the consideration of low-cost and environmentally-friendly copper halides for optoelectronic devices.

**Supporting Information.** Full experimental and computational details, samples photos, single crystal and powder X-ray diffraction results, DSC/TGA, PLQY data, time-resolved PL data, excitation and power dependence PL.

[CCDC 1955726 contains the supplementary crystallographic data for this paper. These data can be obtained free of charge from The Cambridge Crystallographic Data Centre via [www.ccdc.cam.ac.uk/data\\_request/cif](http://www.ccdc.cam.ac.uk/data_request/cif).]

## **ACKNOWLEDGMENTS**

T.C. and A.Y. contributed equally to this work. This work was supported by the University of Oklahoma (OU) startup funds and support from the College of Arts and Sciences at OU. M.-H. Du was supported by the U. S. Department of Energy, Office of Science, Basic Energy Sciences, Materials Sciences and Engineering Division. The UC Santa Barbara Materials Research Lab Shared Experimental Facilities, utilized for confirmatory PLQY measurements, are supported by the MRSEC Program of the NSF under Award No. DMR 1720256; a member of the NSF-funded Materials Research Facilities Network ([www.mrfn.org](http://www.mrfn.org)). We thank Dr. Douglas R. Powell for technical assistance with the single-crystal X-ray diffraction measurements (supported by NSF grant CHE-1726630).

## **Conflict of Interest**

The authors declare no conflict of interest.

## References

- [1] <https://www.energy.gov/eere/ssl/ssl-forecast-report>.
- [2] a) X. Gong, O. Voznyy, A. Jain, W. Liu, R. Sabatini, Z. Piontkowski, G. Walters, G. Bappi, S. Nokhrin, O. Bushuyev, M. Yuan, R. Comin, D. McCamant, S. O. Kelley, E. H. Sargent, *Nat. Mater.* **2018**, *17*, 550; b) J. Xing, Y. Zhao, M. Askerka, L. N. Quan, X. Gong, W. Zhao, J. Zhao, H. Tan, G. Long, L. Gao, Z. Yang, O. Voznyy, J. Tang, Z.-H. Lu, Q. Xiong, E. H. Sargent, *Nat. Commun.* **2018**, *9*, 3541.
- [3] W. Xu, Q. Hu, S. Bai, C. Bao, Y. Miao, Z. Yuan, T. Borzda, A. J. Barker, E. Tyukalova, Z. Hu, M. Kawecki, H. Wang, Z. Yan, X. Liu, X. Shi, K. Uvdal, M. Fahlman, W. Zhang, M. Duchamp, J.-M. Liu, A. Petrozza, J. Wang, L.-M. Liu, W. Huang, F. Gao, *Nat. Photonics.* **2019**, *13*, 418.
- [4] C. Bi, S. Wang, S. V. Kershaw, K. Zheng, T. Pullerits, S. Gaponenko, J. Tian, A. L. Rogach, *Adv. Sci.* **2019**, *6*, 1900462.
- [5] C. Bi, S. Wang, Q. Li, S. V. Kershaw, J. Tian, A. L. Rogach, *J. Phys. Chem. Lett.* **2019**, *10*, 943.
- [6] Y. Liu, J. Cui, K. Du, H. Tian, Z. He, Q. Zhou, Z. Yang, Y. Deng, D. Chen, X. Zuo, Y. Ren, L. Wang, H. Zhu, B. Zhao, D. Di, J. Wang, R. H. Friend, Y. Jin, *Nat. Photonics.* **2019**, doi: 10.1038/s41566-019-0505-4.
- [7] a) R. Roccanova, A. Yangui, H. Nhalil, H. Shi, M.-H. Du, B. Saparov, *ACS Appl. Electron. Mater.* **2019**, *1*, 269; b) R. Roccanova, A. Yangui, G. Seo, T. D. Creason, Y. Wu, D. Y. Kim, M.-H. Du, B. Saparov, *ACS Materials Lett.* **2019**, *1*, 459.
- [8] D. V. Seletskiy, S. D. Melgaard, S. Bigotta, A. Di Lieto, M. Tonelli, M. Sheik-Bahae, *Nat. Photonics.* **2010**, *4*, 161.
- [9] J. Zhang, D. Li, R. Chen, Q. Xiong, *Nature.* **2013**, *493*, 504.
- [10] a) S.-T. Ha, C. Shen, J. Zhang, Q. Xiong, *Nat. Photonics.* **2015**, *10*, 115; b) P. Cai, Y. Huang, H. J. Seo, *J. Phys. Chem. Lett.* **2019**, *10*, 4095.
- [11] Y. V. Morozov, S. Zhang, M. C. Brennan, B. Janko, M. Kuno, *ACS Energy Lett.* **2017**, *2*, 2514.
- [12] Q. Dong, Y. Fang, Y. Shao, P. Mulligan, J. Qiu, L. Cao, J. Huang, *Science.* **2015**, *347*, 967.
- [13] S. Hull, P. Berastegui, *J. Solid State Chem.* **2004**, *177*, 3156.
- [14] M. Sharma, A. Yangui, V. R. Whiteside, I. R. Sellers, D. Han, S. Chen, M.-H. Du, B. Saparov, *Inorg. Chem.* **2019**, *58*, 4446.
- [15] B. Saparov, J.-P. Sun, W. Meng, Z. Xiao, H.-S. Duan, O. Gunawan, D. Shin, I. G. Hill, Y. Yan, D. B. Mitzi, *Chem. Mater.* **2016**, *28*, 2315.
- [16] a) R. Kanno, Y. Takeda, Y. Masuyama, O. Yamamoto, T. Takahashi, *Solid State Ionics.* **1983**, *11*, 221; b) A. Wojakowska, E. Krzyżak, A. Wojakowski, *J. Therm. Anal. Calorim* **2001**, *65*, 491.
- [17] a) C. Zhou, H. Lin, Q. He, L. Xu, M. Worku, M. Chaaban, S. Lee, X. Shi, M.-H. Du, B. Ma, *Mater. Sci. Eng., R.* **2019**, *137*, 38; b) D. Han, H. Shi, W. Ming, C. Zhou, B. Ma, B. Saparov, Y.-Z. Ma, S. Chen, M.-H. Du, *J. Mater. Chem. C.* **2018**, *6*, 6398; c) D. Cortecchia, J. Yin, A. Bruno, S. Z. A. Lo, G. G. Gurzadyan, S. G. Mhaisalkar, J. L. Brédas, C. Soci, *J. Mater. Chem. C.* **2017**, *5*, 2771; d) H. Dammak, A. Yangui, S. Triki, Y. Abid, H. Feki, *J. Lumin.* **2015**, *161*, 214.

- [18] a) V. Morad, Y. Shynkarenko, S. Yakunin, A. Brumberg, R. D. Schaller, M. V. Kovalenko, *J. Am. Chem. Soc.* **2019**, *141*, 9764; b) C. Zhou, H. Lin, M. Worku, J. Neu, Y. Zhou, Y. Tian, S. Lee, P. Djurovich, T. Siegrist, B. Ma, *J. Am. Chem. Soc.* **2018**, *140*, 13181.
- [19] T. Jun, K. Sim, S. Iimura, M. Sasase, H. Kamioka, J. Kim, H. Hosono, *Adv. Mater.* **2018**, *30*, 1804547.
- [20] a) A. Yanguì, D. Garrot, J. S. Lauret, A. Lusson, G. Bouchez, E. Deleporte, S. Pillet, E. Bendeif, M. Castro, S. Triki, Y. Abid, K. Boukheddaden, *J. Phys. Chem. C* **2015**, *119*, 23638; b) A. Yanguì, R. Roccanova, T. M. McWhorter, Y. Wu, M.-H. Du, B. Saparov, *Chem. Mater.* **2019**, *31*, 2983.
- [21] a) S. Li, J. Luo, J. Liu, J. Tang, *J. Phys. Chem. Lett.* **2019**, DOI: 10.1021/acs.jpcclett.8b036041999; b) J. Luo, X. Wang, S. Li, J. Liu, Y. Guo, G. Niu, L. Yao, Y. Fu, L. Gao, Q. Dong, C. Zhao, M. Leng, F. Ma, W. Liang, L. Wang, S. Jin, J. Han, L. Zhang, J. Etheridge, J. Wang, Y. Yan, E. H. Sargent, J. Tang, *Nature* **2018**, *563*, 541.
- [22] a) A. Cowley, B. Foy, D. Danilieu, P. J. McNally, A. L. Bradley, E. McGlynn, A. N. Danilewsky, *Phys. Status Solidi (a)*. **2009**, *206*, 923; b) A. Cowley, Dublin City University, **2012**; c) L. O'Reilly, Dublin City University, **2006**.
- [23] R. K. Vijayaraghavan, D. Chandran, R. K. Vijayaraghavan, A. P. McCoy, S. Daniels, P. J. McNally, *J. Mater. Chem. C* **2017**, *5*, 10270.
- [24] a) B. Saparov, D. B. Mitzi, *Chem. Rev.* **2016**, *116*, 4558; b) R. Roccanova, W. Ming, V. R. Whiteside, M. A. McGuire, I. R. Sellers, M. H. Du, B. Saparov, *Inorg. Chem.* **2017**, *56*, 13878; c) A. Yanguì, S. Pillet, A. Mlayah, A. Lusson, G. Bouchez, S. Triki, Y. Abid, K. Boukheddaden, *J. Chem. Phys.* **2015**, *143*, 224201; d) R. Roccanova, M. Houck, A. Yanguì, D. Han, H. Shi, Y. Wu, D. T. Glatzhofer, D. R. Powell, S. Chen, H. Fourati, A. Lusson, K. Boukheddaden, M.-H. Du, B. Saparov, *ACS Omega*. **2018**, *3*, 18791; e) H. Barkaoui, H. Abid, A. Yanguì, S. Triki, K. Boukheddaden, Y. Abid, *J. Phys. Chem. C* **2018**, *122*, 24253.
- [25] M. Shinada, S. Sugano, *J. Phys. Soc. Jpn.* **1966**, *21*, 1936.
- [26] H. Lin, C. Zhou, Y. Tian, T. Siegrist, B. Ma, *ACS Energy Lett.* **2018**, *3*, 54.
- [27] A. Jain, S. P. Ong, G. Hautier, W. Chen, W. D. Richards, S. Dacek, S. Cholia, D. Gunter, D. Skinner, G. Ceder, K. A. Persson, *APL Mater.* **2013**, *1*, 011002.
- [28] a) Y. V. Morozov, S. Draguta, S. Zhang, A. Cadranet, Y. Wang, B. Janko, M. Kuno, *J. Phys. Chem. C* **2017**, *121*, 16607; b) M. Sheik-Bahae, R. I. Epstein, *Nat. Photonics*. **2007**, *1*, 693; c) M. Sheik-Bahae, R. I. Epstein, *Phys. Rev. Lett.* **2004**, *92*, 247403.
- [29] T. Yamada, T. Aharen, Y. Kanemitsu, *Phys. Rev. Mater.* **2019**, *3*, 024601.
- [30] B. J. Roman, M. T. Sheldon, *Nanophotonics* **2019**, *8*, 599.



## The table of contents

A family of nontoxic all-inorganic halides  $\text{Rb}_2\text{CuX}_3$  ( $\text{X} = \text{Br}, \text{Cl}$ ) was prepared using high temperature and solution techniques. The materials exhibit one-dimensional crystal structures and show high photoluminescence quantum yield blue emission up to unity attributed to self-trapped excitons. Single crystals of  $\text{Rb}_2\text{CuCl}_3$  have also been shown to demonstrate an up-conversion photoluminescence, the first example of such behavior for a Pb-free metal halide.

Authors: T. Creason, A. Yangui, R. Rocanova, A. Strom, M-H. Du, B. Saparov

**Title:** One-Dimensional All-Inorganic Copper Halides with Ultrabright Blue Emission and Up-Conversion Photoluminescence

